

## Phase Relationships and Phase Formation in the System BaF<sub>2</sub>-BaO-Y<sub>2</sub>O<sub>3</sub>-CuO<sub>x</sub>-H<sub>2</sub>O

W. Wong-Ng, L.P. Cook, J. Suh, I. Levin, M. Vaudin, R. Feenstra<sup>1</sup>, and J.P. Cline  
Ceramics Division, National Institute of Standards and Technology  
Gaithersburg, MD 20899, U.S.A

<sup>1</sup>Solid State Division, Oak Ridge National Laboratory  
Oak Ridge, TN 37831, U.S.A.

### ABSTRACT

The interplay of melting equilibria and reaction kinetics is important during formation of the Ba<sub>2</sub>YCu<sub>3</sub>O<sub>6+x</sub> (Y-213) phase from starting materials in the quaternary reciprocal system Ba,Y,Cu//O,F. For experimental investigation of the process we used a combination of differential thermal analysis (DTA) for study of melting equilibria, and in-situ high-temperature x-ray diffraction (HTXRD) for study of the phase formation and reaction kinetics. DTA investigation of compositions spaced along compositional vectors extending from the oxide end to the fluoride end of the reciprocal system have given evidence of low melting liquids (~600 °C) near the fluorine-rich end. Work is continuing to determine whether similar thermal events observed in the interior of the system also indicate low temperature liquids, and on the extent to which low-melting liquids could be involved in Y-213 phase formation. HTXRD investigations have been initiated on the conversion of 0.3 μm and 1.0 μm thick BaF<sub>2</sub>-Y-Cu precursor films to Y-213 in the presence of water vapor. Preliminary results indicated that the thickness of film has a strong influence on the texture of the Y-213 film: a 0.3 μm film showed mainly (001) texture, whereas a 1.0 μm film showed a greater volume fraction of (h00) texture. While the HTXRD method cannot directly reveal the presence of liquid, we are working to combine DTA and HTXRD data for a unified picture of Y-213 phase formation during the “BaF<sub>2</sub> *ex-situ*” process for coated-conductor fabrication.

### INTRODUCTION

The “BaF<sub>2</sub> *ex situ* process”, in which e-beam co-evaporated BaF<sub>2</sub>-Y-Cu-precursor films are deposited on substrates, followed by post-annealing in the presence of H<sub>2</sub>O vapor, has the potential for producing high-quality, long-length, high-J<sub>c</sub>, high T<sub>c</sub> Ba<sub>2</sub>YCu<sub>3</sub>O<sub>6+x</sub> (Y-213) superconductors [1]. The BaF<sub>2</sub> process dates back to 1987, when Mankiewich et al. [2] reported the use of BaF<sub>2</sub> to prepare evaporated precursor films. In the following year, a trifluoroacetate (TFA) method for preparing the precursor was demonstrated by Gupta et al. [3]. In the same year, Chan et al. [4] described a reaction model using H<sub>2</sub>O to decompose the BaF<sub>2</sub>. They also emphasized the importance of removing the product HF for speeding up the reaction. In 1990, McIntyre et al. [5] successfully produced high-J<sub>c</sub>, *c*-axis aligned YBCO coatings by the TFA method. Some beneficial effects of processing under reduced oxygen pressure were also noted [6,7]. They further developed this process during the 90's. In 1991, Feenstra et al. [1] reported on the phase stability of Y-213 at reduced oxygen partial pressure down to 10<sup>-4</sup> atm. Use of

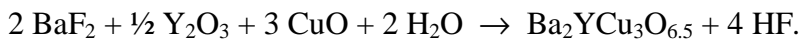
reduced  $p_{O_2}$  allowed lowering of the processing temperature to 700 °C -750 °C. By 1999, Feenstra et al. [8] had demonstrated high- $J_c$   $c$ -axis YBCO on  $CeO_2$  buffer layers. This represented the first successful “coated conductor” application. At about the same time, Solovyov and Suenaga [9] achieved success in preparing thicker (5  $\mu\text{m}$ ) YBCO coatings with high  $J_c$  on single crystal substrates. Recently, Lee [10] showed the feasibility of a continuous process for producing long coated conductor tapes using the  $BaF_2$  *ex-situ* approach.

Today, in order to make the  $BaF_2$  approach commercially viable, it is critical to be able to fully control the process. A complete understanding of the details of the process, including the intermediate phases formed, is also essential for controlling film properties. Several investigators reported that the growth of the Y-213 film could be assisted by the presence of a low-temperature liquid [11, 12]. An amorphous layer (with a Ba:Y:Cu cation ratio of  $\approx 2:1:1.5$ ) between the Y-213 and the untransformed precursor has been observed on intermediate *ex-situ* films (designated as the BNL-films) deposited on  $SrTiO_3$  and  $CeO_2$  substrates at 735 °C [11]. Presence of a low temperature liquid could be important for enhancing the formation of Y-213 through chemical mobility, and also for improving texture of the Y-213 films.

Our overall research objectives are to provide phase equilibrium diagrams needed to optimize processing of Ba-Y-Cu-F-O materials and to assist in the application of this information to coated-conductor processing issues. In particular, it is important to understand the influence of low temperature melts on the formation of the Y-213 phase. The melting was investigated using differential thermal analysis (DTA). High-temperature x-ray diffraction (HTXRD) was used to study the reactions in  $BaF_2$ -Y-Cu precursor films deposited on model  $SrTiO_3$  substrates.

## APPROACH FOR MULTI-DIMENSIONAL PHASE EQUILIBRIA STUDIES

The low-temperature melts were initially studied using the basic quaternary  $BaF_2$ -BaO- $Y_2O_3$ -CuO model system, as shown in Fig. 1 [13]. As water vapor is introduced, ideally the composition of the precursor film, which is shown on the  $BaF_2$ - $Y_2O_3$ -CuO face of the  $BaF_2$ -BaO- $Y_2O_3$ -CuO tetrahedron, migrates through the interior of the tetrahedron, and ultimately arrives at the point corresponding to the 213 superconductor on the base. The overall reaction for the process is



To determine if low melting liquids are involved along this path, we systematically explored the eutectic melting region in the Ba-Y-Cu-O system as a function of oxygen partial pressure, and also with the addition of  $BaF_2$  and  $H_2O$ . The curves in Fig. 2 show the melting temperature of the samples without  $H_2O$  or  $BaF_2$  (from 100 % oxygen to 0.02 % oxygen, by volume) (curve a), and with the presence of both  $H_2O$  and  $BaF_2$  (curve b). Even with the presence of both  $BaF_2$  and  $H_2O$ , the lowest melting temperature was found to be 815 °C at 0.02%  $O_2$ , which is substantially above 735 °C, the temperature at which the amorphous phase was observed in BNL-films [11]. Therefore the low-melting liquid suggested by observations on the BNL-films does not appear to exist as a stable phase in the BaO- $Y_2O_3$ -CuO- $BaF_2$  system under the experimental conditions described, although the possibility of metastable liquids cannot be ruled out [13].

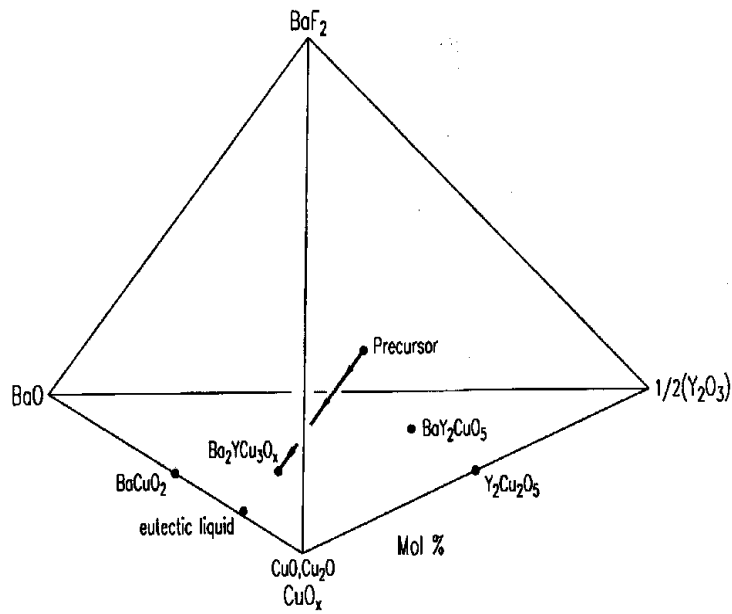


Fig. 1. Quaternary system  $\text{BaF}_2\text{-BaO-Y}_2\text{O}_3\text{-CuO}$ . In the presence of water, the composition of the precursor film migrates through the interior and becomes  $\text{Ba}_2\text{YCu}_3\text{O}_{6+x}$ .

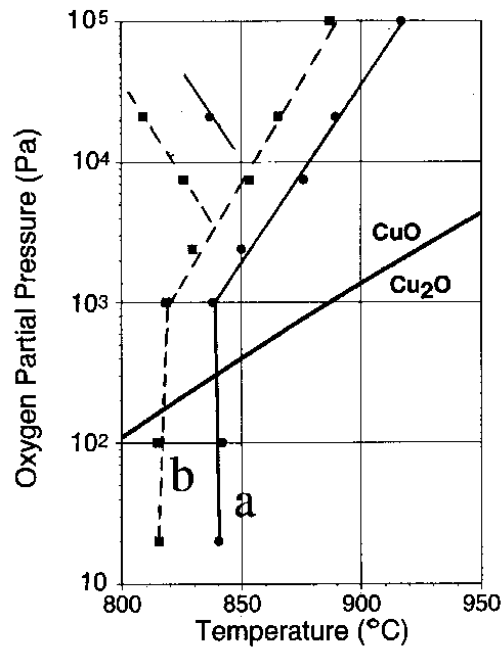


Fig. 2. Eutectic melting in the system  $\text{BaO-Y}_2\text{O}_3\text{-CuO}_x$  at various oxygen partial pressures (a), and with the presence of  $\text{BaF}_2$  and  $\text{H}_2\text{O}$  (b). The  $\text{CuO/Cu}_2\text{O}$  equilibrium is shown for reference.

The possibility that stable liquids more fluorine-rich than the ideal precursor composition might be involved led us to expand our phase equilibrium model to include the full reciprocal Ba,Y,Cu//F,O system (Fig. 3). This system, which can be viewed as a triangular prism with oxides at the base, and corresponding fluorides at the top, consists of three tetrahedra: BaF<sub>2</sub>-BaO-Y<sub>2</sub>O<sub>3</sub>-CuO, BaF<sub>2</sub>-Y<sub>2</sub>O<sub>3</sub>-YF<sub>3</sub>-CuO and YF<sub>3</sub>-CuF<sub>2</sub>-BaF<sub>2</sub>-CuO. Ideally, *ex-situ* precursor films would have a composition plotting on the BaF<sub>2</sub>-Y<sub>2</sub>O<sub>3</sub>-CuO plane; however, if the stoichiometry of these films varies, it is conceivable that oxide/fluoride phase compatibilities in the central or upper portions of the prism could come into play, if only in a transitory manner.

## EXPERIMENTAL

### Phase equilibria

Several of the components of the Ba,Y,Cu//O,F system, most notably BaO and CuF<sub>2</sub>, are atmospherically sensitive, and so all materials were handled under glovebox conditions in an argon atmosphere. Starting materials were reagent grade BaCO<sub>3</sub>, Y<sub>2</sub>O<sub>3</sub>, CuO, CuF<sub>2</sub>, YF<sub>3</sub>, and optical quality single-crystal BaF<sub>2</sub>. BaO was prepared from BaCO<sub>3</sub> by vacuum decomposition. All materials were weighed as fine powders and thoroughly mixed repeatedly with a mortar and pestle. To determine if fluoride-containing compositions having the cation ratios of the Y-213 precursor film (Ba:Y:Cu = 2:1:3) and of the amorphous layer of the BNL-films (Ba:Y:Cu = 2:1:1.5) yield a low-temperature melt, two master batches of fluoride with Ba:Y:Cu of 2:1:3 and 2:1:1.5, and two other batches of oxides with the same cation ratios were prepared. Using these master batches, 20 compositions with different mole fraction ratios of the fluoride and oxide end-members were then prepared along each of the two iso-cationic vectors. Each sample was thus a mixture of three oxides and three fluorides.

An important experimental issue for the study of the Ba,Y,Cu//O,F system concerns container reaction. Although we have generally used MgO crucibles for oxide high-T<sub>c</sub> experiments to minimize container reaction [14], the presence of fluorides presents a different set of problems. For example, MgO reacts with CuF<sub>2</sub> and YF<sub>3</sub> to form MgF<sub>2</sub>. Platinum, frequently a container of choice for fluorides, is known to react with base metal oxides under reducing conditions, and to react with barium oxide under oxidizing conditions. While there is clearly no perfect container material, we have selected platinum as the best compromise under the conditions of our experiments. To monitor the reaction of our Pt DTA cells, we have followed the weight change of the crucibles after each use. It was observed that although the crucibles experienced a slight weight gain during the first usage, subsequent experiments produced only negligible weight change, indicating that after the initial saturation with Ba-Y-Cu, there was essentially no further compositional interaction.

DTA experiments were completed on samples using an electronically upgraded Mettler TA1 system<sup>1</sup> enclosed in an argon-filled glovebox, a feature which eliminated atmospheric contamination during loading of the samples. The system was calibrated against the melting

---

<sup>1</sup> Certain commercial equipment, instruments, or materials are identified in this paper in order to specify the experimental procedure adequately. Such identification is not intended to imply recommendation or endorsement by the National Institute of Standards and Technology, nor is it intended to imply that the materials or equipment identified are necessarily the best available for the purpose.

point of NaCl (801 °C) and the  $\alpha/\beta$  quartz transition (571 °C). During experiments, the samples were surrounded by an atmosphere of flowing gettered argon. After several exploratory experiments, a three-step DTA program was chosen for all 40 compositions and the end members: 1) 25 °C to 950 °C at 10 °C/min (pre-reaction); 2) 950 °C to 450 °C at 10 °C/min (cooling); 3) 450 °C to 1150 °C at 10 °C/min (measurement). This sequence resulted in reaction of the unstable starting combinations during step 1, as evidenced by strong exotherms at <500 °C for most compositions. During cooling step 2, exotherms were interpreted as indicating presence of melt, which was generally confirmed by corresponding endotherms on subsequent heating during step 3.

## **High-temperature x-ray powder diffraction studies**

### **(1) Film deposition**

The “BaF<sub>2</sub>” precursor films were prepared by electron beam evaporation of Cu and Y metal and BaF<sub>2</sub> compound as described in [1]. The substrates were not intentionally heated during the deposition. Two sets of films with thickness of 0.3  $\mu\text{m}$  and 1  $\mu\text{m}$ , respectively, were deposited on SrTiO<sub>3</sub> as the model substrate. The (100) SrTiO<sub>3</sub> substrates were annealed at 1000 °C in 1 atm of O<sub>2</sub> prior to the precursor deposition [1].

### **(2) X-ray diffractometer**

A high-temperature Siemens 5000  $\theta$ - $\theta$  x-ray diffractometer system, equipped with a scintillation counter and a high-temperature furnace, was modified for the present study by adding a gas flow apparatus. This apparatus included a series of bubblers containing NaCl-saturated water at room temperature, and an oxygen analyzer. Helium gas containing ~ 200 ppm O<sub>2</sub> by vol. was flowed through the bubblers and passed directly over the sample in the enclosed furnace chamber. Because of the  $\theta$ - $\theta$  geometry, the specimen remained fixed in a horizontal position during experiments. Cu K $_{\alpha}$  radiation was used for the studies.

The 0.3  $\mu\text{m}$  BaF<sub>2</sub> film (E-1) was heated from room temperature to 735 °C over a 2 h period. A thicker 1  $\mu\text{m}$  film (W-1) was ramped up to 735 °C in 30 minutes. Since the crystallization of BaF<sub>2</sub> and the defluorination reactions take place at a relatively rapid rate, continuous high temperature x-ray measurements were performed within a small  $2\theta$  range of 12°.

## **RESULTS AND DISCUSSION**

### **Phase equilibria**

Figure 3 shows the two composition vectors that correspond to the cation ratios Ba:Y:Cu = 2:1:3 and Ba:Y:Cu = 2:1:1.5. From the base triangle to the top, compositions vary from the oxide-rich to the fluoride-rich end. The minimum melting temperatures of these samples were measured by DTA. Figure 4 shows the plot of the DTA temperatures vs. mole fraction of the end-member oxide and fluoride for Ba:Y:Cu = 2:1:3. With progression along the 2:1:3 vector, the bulk compositions pass successively through each of the constituent tetrahedrons of Fig. 3. For example, the compositions in section 1 of Fig. 4 correspond to the compositions in the

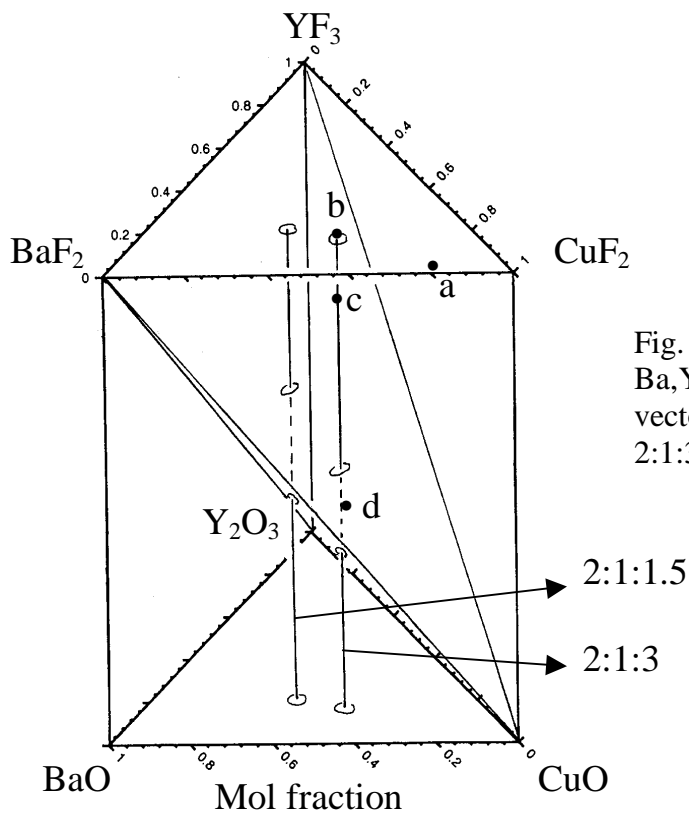
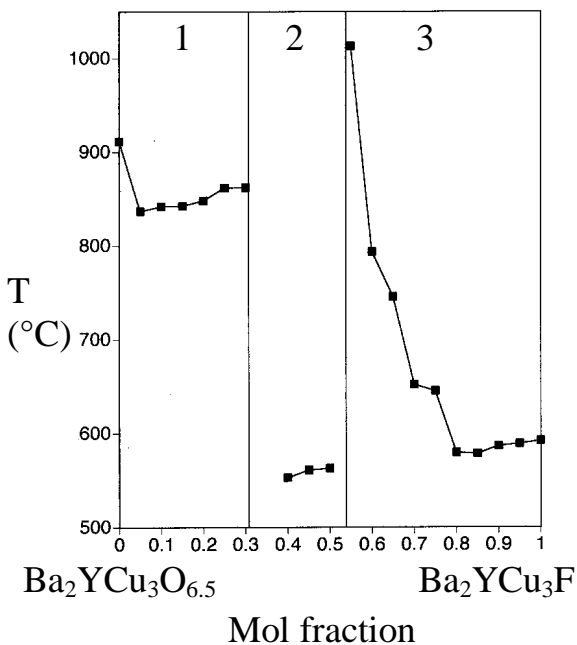
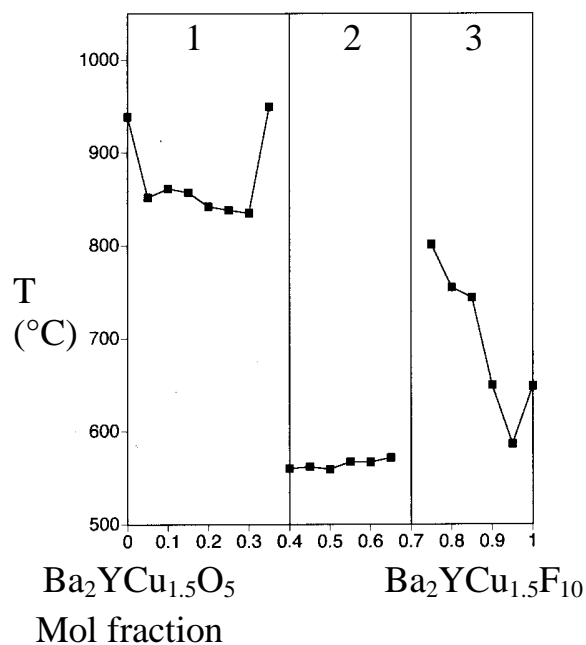


Fig. 3. Full reciprocal system Ba,Y,Cu//O,F. Two compositional vectors with Ba:Y:Cu = 2:1:3 and 2:1:1.5 are illustrated.



$Ba_2YCu_3O_{6.5}$   $Ba_2YCu_3F$   
Mol fraction

Fig. 4. DTA temperatures as a function of mole fraction of fluoride end-member along the Ba:Y:Cu = 2:1:3 composition vector.



$Ba_2YCu_{1.5}O_5$   $Ba_2YCu_{1.5}F_{10}$   
Mol fraction

Fig. 5. DTA temperatures as a function of mole fraction of fluoride end-member along the Ba:Y:Cu = 2:1:1.5 composition vector.

tetrahedron BaO-BaF<sub>2</sub>-Y<sub>2</sub>O<sub>3</sub>-CuO. The DTA temperatures of the compositions in section 1 are relatively high, in the 800 °C - 900 °C range. However, in sections 2 and 3 (BaF<sub>2</sub>-Y<sub>2</sub>O<sub>3</sub>-YF<sub>3</sub>-CuO and YF<sub>3</sub>-CuF<sub>2</sub>-BaF<sub>2</sub>-CuO tetrahedra), an abrupt lowering of the DTA temperatures to less than 600 °C was observed. In Fig. 5, a similar trend of the DTA temperatures along the Ba:Y:Cu = 2:1:1.5 vector (amorphous layer of the BNL-film) was observed. Therefore possible low melting events may take place in the interior, as well as in the top tetrahedron of the Ba,Y,Cu//F,O system. The melting of compositions in the BaF<sub>2</sub>-CuF<sub>2</sub>, BaF<sub>2</sub>-CuF<sub>2</sub>-YF<sub>3</sub>, BaF<sub>2</sub>-CuF<sub>2</sub>-YF<sub>3</sub>-CuO, and BaF<sub>2</sub>-Y<sub>2</sub>O<sub>3</sub>-YF<sub>3</sub>-CuO systems is currently undergoing further study.

The binary BaF<sub>2</sub>-CuF<sub>2</sub> system was investigated by Samouel et al. [15], and a low-melting eutectic liquid was reported below 620 °C at 27.5 mole fraction % BaF<sub>2</sub>. Our experiments have confirmed the existence of this low-melting liquid. The optical micrograph of a sample of the eutectic composition (composition (a) in Fig. 3) which was heat-treated at 650 °C in the DTA apparatus is shown in Fig. 6.

The initial melt temperature for composition (b) in the BaF<sub>2</sub>:YF<sub>3</sub>:CuF<sub>2</sub> system (Fig. 3, end point of the Ba:Y:Cu = 2:1:3 composition line) was determined by DTA to be 592 °C, which is slightly lower than the binary eutectic temperature of 617 °C in the BaF<sub>2</sub>-CuF<sub>2</sub> system. Within the YF<sub>3</sub>-CuF<sub>2</sub>-BaF<sub>2</sub>-CuO tetrahedron, the temperature of the DTA thermal event for composition (c), with an oxide/fluoride ratio of 15/85, further lowers to 578 °C. In general, the melts of the interior fluoride-oxide systems are not as easy to observe as the cuprate type liquids in the BaO-Y<sub>2</sub>O<sub>3</sub>-CuO system, which are dark and readily creep up the sides of the crucible. Figure 7 shows an optical micrograph of the Pt-crucible which contains a sintered sample from loose powder of composition (b) at 700 °C. Surrounding the pellet, an area interpreted as recrystallized melt can be detected.

Based on an observed DTA event at 576 °C, a sample of composition (d) in the BaF<sub>2</sub>-Y<sub>2</sub>O<sub>3</sub>-YF<sub>3</sub>-CuO tetrahedron, with an oxide/fluoride ratio of 45/55 along the 2:1:1.5 vector was homogenized at 950 °C, cooled to 450 °C, reground and annealed at 650 °C. An optical micrograph of the resulting sample is shown in Fig. 8. At 650 °C, a somewhat sintered sample is possibly the result of the presence of a small amount of liquid, which aids the sintering process. At present, it is not certain if this low temperature thermal event corresponds to melting; investigation continues.

To determine if reduced copper may affect the presence of liquid, we performed a DTA experiment using composition (d) but replacing CuO with Cu<sub>2</sub>O. While the DTA onset temperature was also observed at around 567 °C, the size of the DTA peak appears to be much larger, possibly indicating a larger quantity of melt. From these observations, we infer that the low-melting liquid may be reduced relative to CuO, and that its presence may be favored by lower *p*<sub>O<sub>2</sub></sub>. Fig. 9 shows the interior of the Pt crucible after a melting experiment at 1150 °C with the Cu<sub>2</sub>O-based starting material. A white scale seen peeling from the crucible walls and encrusting the residual crystalline material is interpreted as evidence of liquid. The textural features suggest that the liquid has a relatively low surface tension.

The low-temperature melts that have been determined so far appear to have a greater fluorine content than the composition on the BaF<sub>2</sub>-Y<sub>2</sub>O<sub>3</sub>-CuO plane. A composition removed from this plane towards the fluorine-rich direction (mid- and top-level tetrahedra) due to local inhomogeneity will give a low-temperature melt. It is possible that the amorphous layer observed in the BNL-film was produced by a liquid that was originally relatively fluorine rich, and subsequently it was defluorinated during reaction with H<sub>2</sub>O.

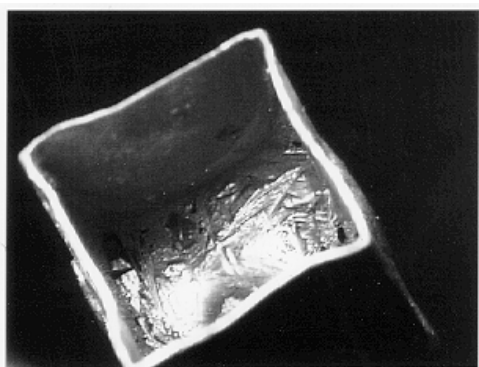


Fig. 6. Optical micrograph of composition (a) in Fig. 3 ( $\text{BaF}_2\text{:CuF}_2 = 27.5\text{:}72.5$ ) heated at  $620\text{ }^\circ\text{C}$ . Melting was observed.

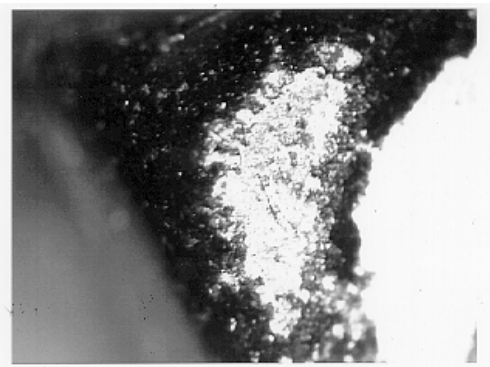


Fig. 7. Optical micrograph of composition (c) in Fig. 3 (in the  $\text{YF}_3\text{-CuF}_2\text{-BaF}_2\text{-CuO}$  subsystem) heated at  $700\text{ }^\circ\text{C}$ . Recrystallized melt can be observed.



Fig. 8. Optical micrograph of composition (d) in Fig. 3 (in the  $\text{BaF}_2\text{-Y}_2\text{O}_3\text{-YF}_3\text{-CuO}$  subsystem) heated at  $650\text{ }^\circ\text{C}$ .

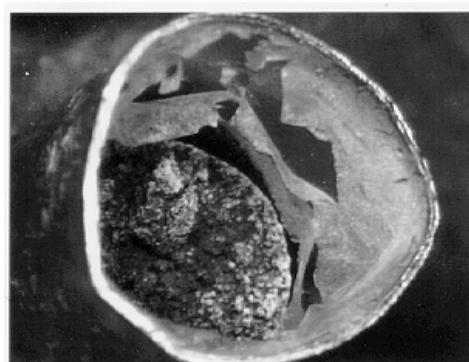


Fig. 9. Optical micrograph of composition (d) in Fig. 3 (in the  $\text{BaF}_2\text{-Y}_2\text{O}_3\text{-YF}_3\text{-CuO}$  subsystem) heated at  $1150\text{ }^\circ\text{C}$  (using  $\text{Cu}_2\text{O}$ ).

## **High-temperature x-ray diffraction studies**

Figure 10 is a series of selected high temperature x-ray patterns ( $12^\circ$  range  $2\theta$ ) from the  $0.3\ \mu\text{m}$  E-1 film showing the crystallization of the  $\text{BaF}_2$  type phase and the formation of Y-213. The formation of Y-213 is evidenced from the increasing intensity of the  $00l$  peaks as the temperature increases. The x-ray pattern of the E-1 film after cooling to room temperature from  $735\ ^\circ\text{C}$  is shown in Fig. 11. This pattern is dominated by  $00l$  peaks of Y-213 (plus small  $h00$  peaks).

Figure 12 illustrates selected x-ray patterns of the thicker W-1 ( $1\ \mu\text{m}$ ) film. The evolution of the  $002$  peak of the 213 phase can be detected from these patterns. Fig. 13 is a plot of the intensity of the strongest  $\text{BaF}_2$  peak ( $111$ ) and the  $002$  peak of the Y-213 phase as a function of time in minutes. The zero time corresponds to the maximum intensity of the  $\text{BaF}_2$  peak. As expected, the peak intensity of  $\text{BaF}_2$  decreases as the amount of Y-213 increases, and the maximum amount of Y-213 occurs at the time when  $\text{BaF}_2$  totally disappears. The precursor appears to be fully converted to Y-213 in about 100 minutes. In the x-ray pattern of the W-1 film after cooling to room temperature from  $735\ ^\circ\text{C}$  (Fig. 14), the  $h00$  peaks appear to be stronger than the  $00l$  peaks. In addition, other peaks due to random orientation such as  $102$ ,  $103$  and  $110$  also appear.

The epitaxial growth of these two films was characterized by  $\omega$ -scans using the  $007$  and  $200$  Y-213 reflections. The full width half-maximum (FWHM) using the  $007$  peak is the same on both films ( $0.64^\circ$ ), and is relatively narrow, indicating near-epitaxy in both films. The FWHM of the  $200$  peak of the W-1 film is very narrow,  $0.34^\circ$ , indicating a very sharp  $a$ -axis texture.

As a summary, the x-ray diffraction results showed that the E-1 film has mainly  $00l$ -texturing and a smaller volume fraction of  $100$  texturing. The thicker  $1\ \mu\text{m}$  film shows a larger volume fraction of  $(100)$  texturing than  $(00l)$ , together with regions of randomly oriented grains.

## **SUMMARY**

We have presented evidence for regions of low melting liquids of below  $600\ ^\circ\text{C}$ , on the fluorine rich side of the  $\text{BaF}_2\text{-Y}_2\text{O}_3\text{-CuO}$  plane in the  $\text{Ba,Y,Cu//F,O}$  reciprocal system. These liquids may be favored by reduced  $p_{\text{O}_2}$ , and are possibly correlated with the observations made during *ex-situ* processing of the BNL-films. If so, the presence of such liquids may be subject to manipulation by careful control of  $p_{\text{O}_2}$  and film stoichiometry. Further characterization of the liquid compositions will be made using quantitative energy dispersive x-ray spectroscopy (EDS). Future high temperature x-ray studies using a position-sensitive detector will allow us to expand the  $2\theta$  range and to obtain patterns in a much shorter time. Analysis of phases which are present prior to and simultaneously with Y-213 will reveal phase formation sequence.

## **ACKNOWLEDGEMENTS**

This work has been partially supported by the U.S. Department of Energy. The authors have benefitted from discussions with Dr. M. Suenaga of Brookhaven National Laboratory. Dr. Jonathan Storer of 3M Corporation provided the single crystal  $\text{BaF}_2$  used as starting material.

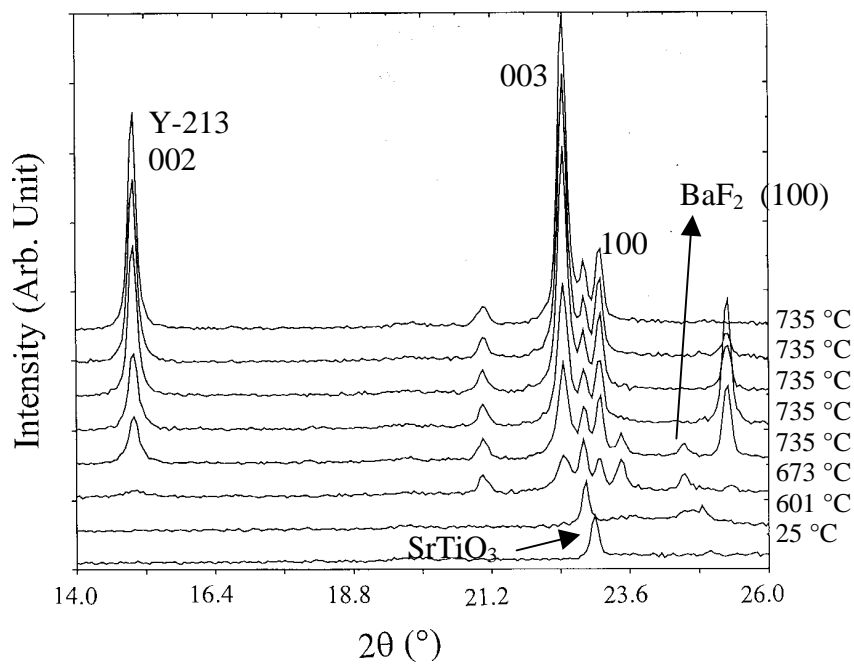


Fig. 10. High temperature x-ray diffraction patterns of film E-1 (0.3 μm). The film was heated up to 735 °C in 2 hr.

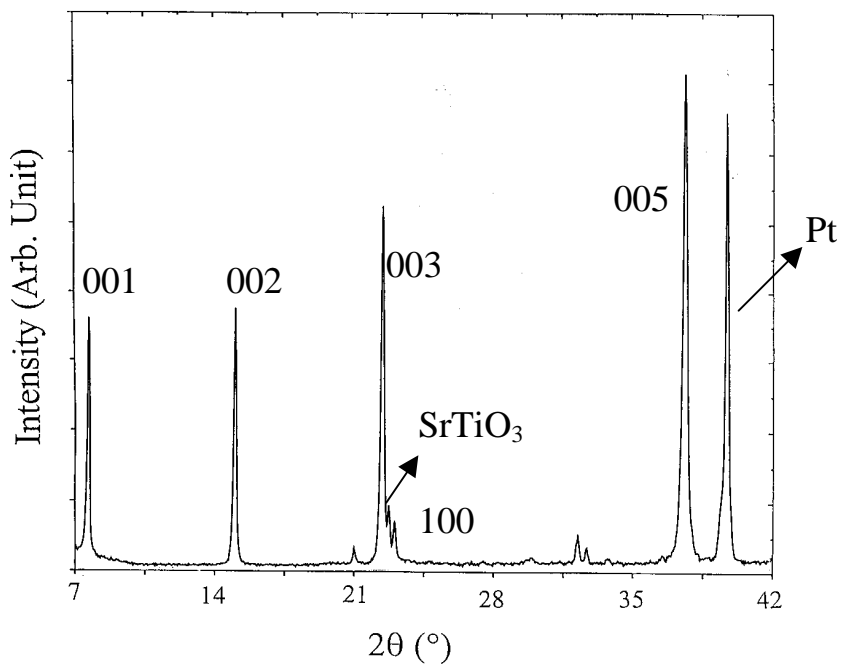


Fig. 11. X-ray diffraction pattern of film E-1 after cooling from 735 °C to room temperature.

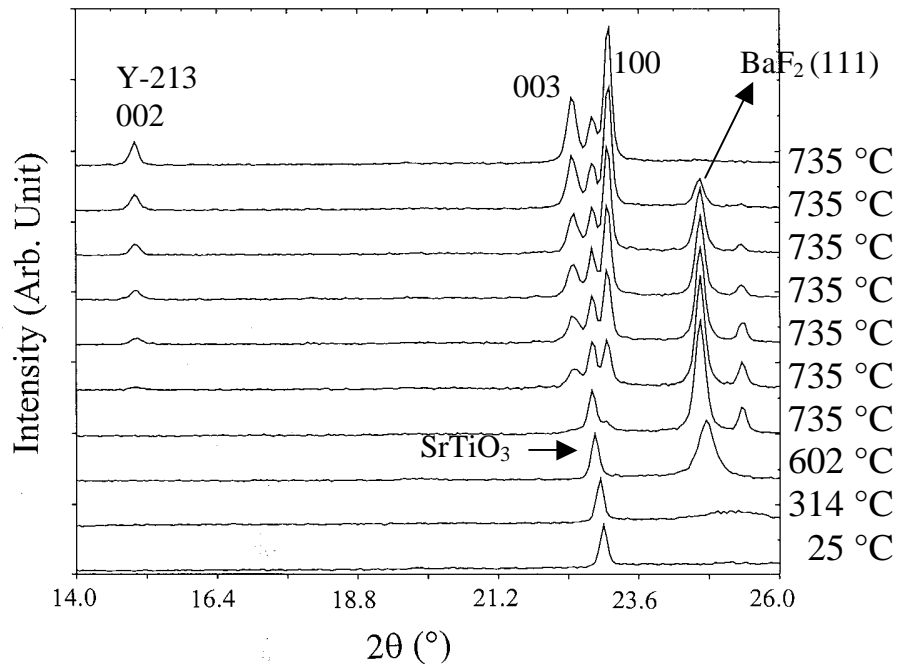


Fig. 12. High temperature x-ray diffraction patterns of film W-1 (1  $\mu\text{m}$ ). The film was heated up to 735 °C in 30 min.

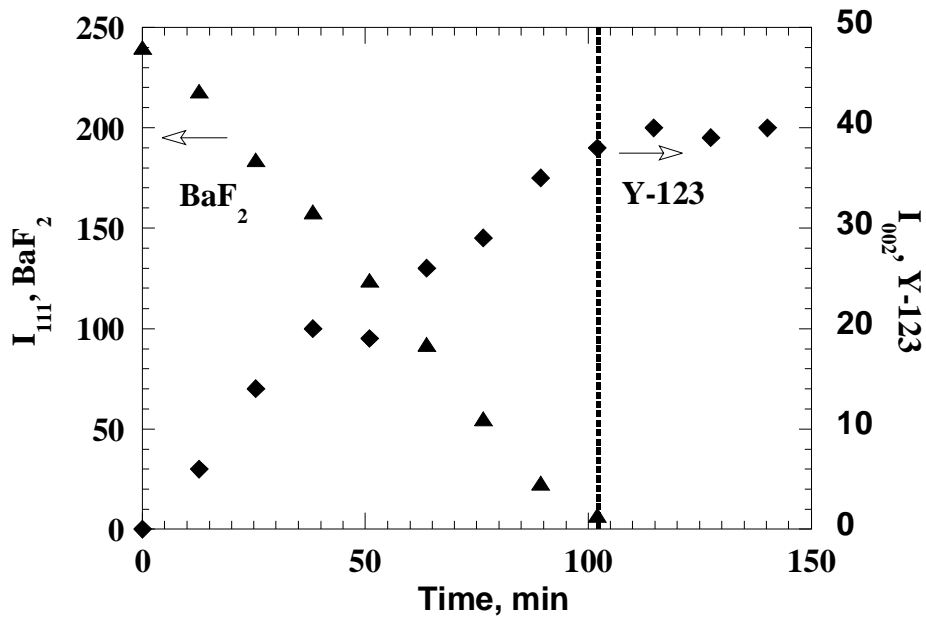


Fig. 13. A plot of the integrated intensity of the strongest BaF<sub>2</sub> (111) peak and the Y-213 (002) peak for film W-1 as a function of time (min)

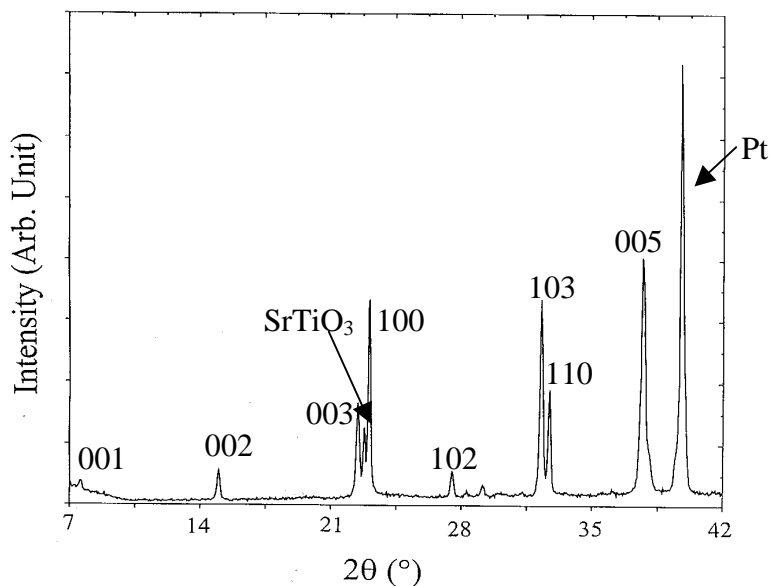


Fig. 14. X-ray diffraction pattern of film W-1 after cooling from 735 °C to room temperature.

## REFERENCES

1. R. Feenstra, T. B. Lindemer, J. D. Budai, and M. D. Galloway, *J. Appl. Phys.* **69**, 6569 (1991).
2. P.M. Mankiewich, J.H. Scofield, W.J. Skocpol, R.E. Howard, A.H. Dayem, and E. Good, *Appl. Phys. Lett.* **51** (21) 1753 (1987).
3. A. Gupta, R. Jagannathan, E.I. Cooper, E.A. Giess, J.I. Landman, and B.W. Hussey, *Appl. Phys. Lett.* **52** (24), 2077 (1988).
4. S.-W. Chan, B.G. Bagley, L.H. Greene, M. Giroud, W.L. Feldmann, K.R. Jenkin, II, and B.J. Wilkins, *Appl. Phys. Lett.* **53** (15) 1443 (1988).
5. P.C. McIntyre and M. Cima, *J. Mater. Res.* **5**, 4183 (1990).
6. P.C. McIntyre, M. J. Cima, and A. Roshko, *J. Appl. Phys.* **77** (10) 5263 (1995).
7. P.C. McIntyre, M. J. Cima, J.A. Smith, Jr., R.B. Hallock, M.P. Siegal, and J.M. Phillips, *J. Appl. Phys.* **71** 1868 (1992).
8. R. Feenstra, US Patent 5,972,847 (1999).
9. V.F. Solovyov and M. Suenaga, *Physica C* **309**, 269 (1998).
10. D.F. Lee, DOE Peer Review, Washington DC, July, 2000.
11. L. Wu, Y. Zhu, V.F. Solovyov, H.J. Weismann, A.R. Moodenbaugh, R.L. Sabatini, and M. Suenaga, in press, 2001.
12. P.C. McIntyre, M. J. Cima, *J. Mater. Res.* **9** 2219 (1994).
13. L.P. Cook, W. Wong-Ng and J. Suh in *High-Temperature Superconductors – Crystal Chemistry, Processing and Properties*, edited by U. Balachandran, H.C. Freyhardt, T. Izumi, and D.C. Labalestier (Mater. Res. Soc. Proc. **659**, Pittsburg, PA, 2001) pp. II4.8.1 (2001).
14. W. Wong-Ng and L. P. Cook, *J. Res. Natl. Inst. Stand. Technol.* **103**, 379 (1998).
15. M. Samouel, *C.R. Acad.Sci. Ser. C* **270** [22] 1805 (1970).